International Journal of Science Engineering and Advance Technology

Simulation of SVPWM Based Multivariable Control Method for a DFIG Wind Energy System

G. SWATHI
P.G. scholar, Dept of EEE
QIS Institute of Technology
Ongole, Andhra Pradesh, India

Prof. O.V.S. SRINIVASA PRASAD
Head of the Dept, EEE
QIS Institute of Technology
Ongole, Andhra Pradesh, India

A. VENKATA SURESH
Associate professor
QIS Institute of Technology
Ongole, Andhra Pradesh, India

Abstract — **This paper deals with a variable speed device to produce electrical energy on a power network based on a doubly-fed induction machine used in generating mode (DFIG) in wind energy system by using SVPWM power transfer matrix. This paper presents a modeling and control approach which uses instantaneous real and reactive power instead of dq components of currents in a vector control scheme. The main features of the proposed model compared to conventional models in the dq frame of reference are robustness and simplicity of realization. The sequential loop closing technique is adopted to design a multivariable control system including six compensators for a DFIG wind energy system to capture the maximum wind power and to inject the required reactive power to the generator. In this paper SVPWM method is used for better controlling of converters. It also provides fault ride through method to protect the converter during a fault. The time-domain simulation of the study system is presented by using MATLAB Simulink to test the system robustness, to validate the proposed model and to show the enhanced tracking capability.**

I. INTRODUCTION

Wind energy, known as a kind of clean and environmental-friendly energy, has gained world-wide attention in the last decades. At present, the penetration of wind energy into the power system is increasing rapidly. Among various alternatives to construct grid-connected wind turbines, the ones based on doubly fed induction generators (DFIGs) are dominating the energy market due to their outstanding merits, including competitive durability, lower converter cost, and flexible power control, compared with other solutions such as fixed-speed induction generators or the ones with fully rated converter systems [1-3]. However, owing to direct connections between stator windings and the grid and limited power rating of the rotor side excitation converter, the DFIG-based wind turbine systems have been found to be more sensitive and vulnerable to grid disturbances. Hence, the issues in power quality, faultride- through (FRT) capability, and reactive power compensation based on DFIG systems have attracted more and more attention recently Wind energy systems based on doubly fed induction generators (DFIGs) have been dominantly used in high-power applications since they use power-electronic converters with ratings less than the rating of the wind turbine generators [3]–[5]. The scope of this paper is analysis of dynamic modeling and control of DFIG wind turbine generators.

Conventionally we are having stator field oriented control/vector control [4-5] and direct torque control for the DFIG controlling. The vector control uses the dq frame to control the current components for real/reactive power of the machine. The unavailable dq forms causes here to compute abc/dq0 transformation using a phased lock loop [7].

The dynamics of abc/qd0 transformations are often ignored in the procedure of control design. Thus, any control design approach must be adequately robust to overcome the uncertainties in estimation of machine parameters as well as unaccounted dynamics of the overall system. The proposed power transfer matrix model for DFIG in this paper presents an alternative modeling and control approach which is independent of abc/qd0 transformations.

Direct torque control (DTC) and direct power control schemes (DPC) have been presented as alternative methods which directly control machine flux and torque via the selection of suitable voltage vectors. It has been shown that DPC is a more efficient approach compared to modified DTC [12]. However, the DPC method also depends on the estimation of machine parameters and it requires a protection mechanism to avoid over current during a fault in the system. This paper presents a modeling and control approach which uses instantaneous real and reactive power instead of dq components of currents in a vector control

scheme. The main features of the proposed model compared to conventional models in the dq frame of reference are as follows.

1) *Robustness:* The waveforms of power components are independent of a reference frame; therefore, this approach is inherently robust against unaccounted dynamics such as PLL.

2) *Simplicity of realization:* The power components (state variables of a feedback control loop) can be directly obtained from phase voltage/current quantities, which simplifies the implementation of the control system.

Using power components instead of current in the model of the system, the control system requires an additional protection algorithm to prevent over current during a fault. Such an algorithm can be simply added to the control system via measuring the magnitude of current. The sequential loop closing technique is adopted to design a multivariable control system including six compensators for a DFIG wind energy system. The designed control system captures maximum wind power via adjusting the speed of the DFIG and injects the required reactive power to the system via a grid-side converter [11-18].

II. DFIG MODELING OF A WIND ENERGY SYSTEM

A. *Structure of a DFIG in wind energy*

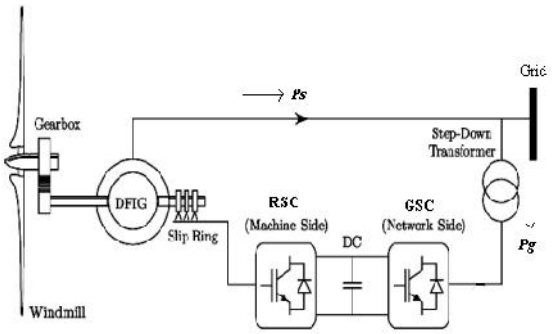

Fig. 1. Model of a dfig wind turbine

The model of a DFIG wind turbine is depicted in Fig. 1. It consists of a wind turbine which is connected to grid by a DFIG via transmission network. The two power converters of DFIG's are RSC (Rotor side converter) and GSC (grid side converter). RSC used to control the speed of the generator and GSC used to control the grid/network side real/reactive power. The instantaneous real and reactive power components of the grid-side converter, $p_g(t)$ and $q_g(t)$, in the synchronous dq reference frame, are [18]

$$\begin{bmatrix} p_g(t) \\ q_g(t) \end{bmatrix} = \frac{3}{2}\begin{bmatrix} v_{sd} & v_{sq} \\ v_{sq} & -v_{sd} \end{bmatrix}\begin{bmatrix} i_{gd} \\ i_{gq} \end{bmatrix} \quad (1)$$

Where $v_{sd,sq}$ and $i_{gd,gq}$ are components of the stator voltages and GSC currents in the synchronous reference frame, respectively. Solving (1) for i_{gd} and i_{gq}, we obtain

$$\begin{bmatrix} i_{gd} \\ i_{gq} \end{bmatrix} = K_v \begin{bmatrix} p_g(t) \\ q_g(t) \end{bmatrix} \quad (2)$$

Where

$$K_v = \frac{2}{3v_s^2}\begin{bmatrix} v_{sd} & v_{sq} \\ v_{sq} & -v_{sd} \end{bmatrix}, |v_s| = \sqrt{v_{sq}^2 + v_{sd}^2}. \quad (3)$$

The instantaneous real/reactive power components of DFIG of stator currents are given by

$$\begin{bmatrix} p_g(t) \\ q_g(t) \end{bmatrix} = -\frac{3}{2}\begin{bmatrix} v_{sd} & v_{sq} \\ v_{sq} & -v_{sd} \end{bmatrix}\begin{bmatrix} i_{gd} \\ i_{gq} \end{bmatrix}$$

and the stator current components are given by

$$\begin{bmatrix} i_{sd} \\ i_{sq} \end{bmatrix} = -K_v \begin{bmatrix} p_s(t) \\ q_s(t) \end{bmatrix} \quad (4)$$

The negative sign in (4) indicates the direction of the stator power flow.

The voltage and torque equations are utilized to model the dynamic model of DFIG [3]. Herein, we develop a simplified model for the DIFG-based wind turbine of Fig. 1 by substituting currents in the exact model in terms of instantaneous real and reactive power. The key assumption to simplify the model is assuming an approximately constant stator voltage for DFIG. This assumption can be only used under a steady-state condition where the grid voltage at the point of common coupling (PCC) varies in a narrow interval, typically less than 0.05 p.u. Using this assumption, is K_v approximately constant and derivatives of currents will be proportional to the derivatives of power based on (2) and (4).

B. Model of DFIG

The model of DFIG uses instantaneous power components. The voltage and flux equations of a doubly fed induction machine in the stator voltage synchronous reference frame can be summarized as

$$V_{sdq} = r_s i_{sdq} + j\omega_{sl}\psi_{rdq} + \frac{d\psi_{sdq}}{dt} \quad (5)$$

$$V_{rdq} = r_r i_{rdq} + j\omega_{sl}\psi_{rdq} + \frac{d\psi_{rdq}}{dt} \quad (6)$$

$$\psi_{sdq} = L_s i_{sdq} + L_m i_{rdq},\ \psi_{rdq} = L_m i_{sdq} + L_r i_{rdq} \quad (7)$$

Where r_s and r_r are the stator and rotor resistances, and is the synchronous (stator) frequency. Subscripts and signify the stator and rotor variable and L_s, L_r and L_m are the stator, rotor, and magnetization inductances, respectively. The complex quantities v_{dq}, i_{dq} and ψ_{dq} represent the voltage, current, and flux vectors, and ω_{sl} is the slip frequency defined as

$$\psi_{sdq,rdq} \triangleq \psi_{sd,rd} + j\psi_{sq,rq}, \omega_{sl} \triangleq \omega_e - \omega_r$$

where ω_r is the rotor speed of the induction machine. To obtain a model of DFIG in terms of $p(t)$ and $q(t)$, the rotor flux and current are obtained from (7) as

$$i_{rdq} = \frac{\psi_{sdq} - L_s i_{sdq}}{L_m}, \psi_{rdq} = \frac{L_r}{L_m}\left(\psi_{sdq} - L'_s i_{sdq}\right) \quad (8)$$

Where $L'_s \triangleq \left(1 - (L_m^2)/(L_s L_r)\right)L_s$.

Then, by substituting for i_{rdq} and v_{rdq} from (8) in (6) and then by solving (5) and (6) for i_{sdq}, we obtain

$$\frac{d}{dt} i_{sdq} = \frac{1}{L'_s} v_{sdq} - \frac{L_m}{L'_s L_r} v_{rdq} + \frac{r_r - j\omega_r L_r}{L'_s L_r} \psi_{sdq}$$

$$- \left(\frac{r_r L_s + r_s L_r}{L_r L'_s} + j\omega_{sl}\right) i_{sdq} \quad (9)$$

Using (4) to replace $i_{sd,sq}$ components of i_{sdq} in (9) and by rearranging the equation, we obtain

$$\frac{dp_s}{dt} = g_1 p_s - \omega_{sl} q_s - g_4 \psi_{sd} - g_5 \psi_{sq} + u_{rd} \quad (10)$$

$$\frac{dq_s}{dt} = \omega_{sl} p_s + g_1 q_s - g_5 \psi_{sd} + g_4 \psi_{sq} + u_{rq} \quad (11)$$

Where

$$u_{rd} = g_2 v_{rd} + g_3 v_{rq} - \frac{3|v_s|^2}{2L'_s}$$

$$u_{rq} = g_3 v_{rd} - g_2 v_{rq}, g_1 = -\frac{r_s L_r + L_s r_s}{L'_s L_r},$$

$$g_2 = \frac{3L_m v_{sd}}{2L_r L'_s}$$

$$g_3 = \frac{3L_m v_{sq}}{2L_r L'_s}, g_4 = \frac{3}{2}\left(\frac{r_r v_{sd} - L_s \omega_r v_{sq}}{L'_s L_r}\right)$$

$$g_5 = \frac{3}{2}\left(\frac{r_r v_{sq} - L_r \omega_r v_{sd}}{L'_s L_r}\right)$$

The state equation of the stator flux can be obtained by substituting for i_{sq} and i_{sd} from (4) in (5). Solving the stator voltage equations for $\psi_{sd,sq}$ yields

$$\frac{d\psi_{sd}}{dt} = v_{sd} + \omega_e \psi_{sq} + \frac{2r_s}{3|v_s|^2}\left(v_{sd} p_s + v_{sq} q_s\right) \quad (12)$$

$$\frac{d\psi_{sq}}{dt} = v_{sq} + \omega_e \psi_{sd} + \frac{2r_s}{3|v_s|^2}\left(v_{sq} p_s - v_{sd} q_s\right) \quad (13)$$

The electromechanical dynamic model of the machine is

$$\frac{d\omega_r}{dt} = \frac{P}{J}(T_e - T_m) \quad (14)$$

where P, J and T_m are the number of pole pairs, inertia of the rotor, and mechanical torque of the machine, respectively. The electric torque is given by

$$T_e = \frac{3}{2} P\left(\psi_{sd} i_{sq} - \psi_{sq} i_{sd}\right) \quad (15)$$

In (14), the mechanical torque T_m is input to the model and T_e, based on (15), can be expressed in terms of instantaneous real and reactive power. Substituting for i_{sd} and i_{sd} from (4) in (15) and then replacing T_e in (14), we deduce

$$\frac{d\omega_r}{dt} = g_6 p_s + g_7 q_s - \frac{P}{J} T_m \quad (16)$$

Where

$$g_6 = \frac{P^2}{J}\frac{\psi_{sq} v_{sd} - \psi_{sd} v_{sq}}{v_s^2}, \; g_7 = \frac{P^2}{J}\frac{\psi_{sd} v_{sd} + \psi_{sq} v_{sq}}{v_s^2}.$$

The simplified model of the induction machine is presented in (10)–(13) and (16) which is summarized as

$$\frac{d}{dt}\begin{bmatrix} p_s \\ q_s \\ \psi_{sd} \\ \psi_{sq} \\ \omega_r \end{bmatrix} = \begin{bmatrix} g_1 & -\omega_{sl} & -g_4 & -g_5 & 0 \\ \omega_{sl} & g_1 & -g_5 & g_4 & 0 \\ \frac{2r_s v_{sd}}{3|v_s|^2} & \frac{2r_s v_{sq}}{3|v_s|^2} & 0 & \omega_e & 0 \\ \frac{2r_s v_{sq}}{3|v_s|^2} & -\frac{2r_s v_{sd}}{3|v_s|^2} & -\omega_e & 0 & 0 \\ g_6 & g_7 & 0 & 0 & 0 \end{bmatrix}$$

$$X \begin{bmatrix} p_s \\ q_s \\ \psi_{sd} \\ \psi_{sq} \\ \omega_r \end{bmatrix} + \begin{bmatrix} u_{rd} \\ u_{rq} \\ v_{sd} \\ v_{sq} \\ \frac{PT_m}{-J} \end{bmatrix}. \quad (17)$$

The model of DFIG in (17) is a nonlinear dynamic model since the coefficients of the state variables are functions of the state variables.

C. Model of GSC and Filter

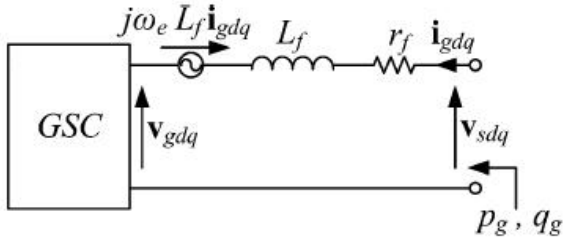

Fig.2. Filter Equivalent circuit

The equivalent representation of grid side filter is as shown in fig. 2. The dq model of the grid-side converter and filter is

$$V_{sdq} = V_{gdq} + L_f \frac{di_{gdq}}{dt} + j\omega_e L_f i_{gdq} + r_f i_{gdq} \quad (18)$$

Where r_f and L_f are the resistance and inductance of the filter, respectively, and subscript signifies the variables at the grid side converter [16]. Substituting for i_{gdq} from (2) in (18) yields

$$\begin{bmatrix} \frac{dp_g}{dt} \\ \frac{dq_g}{dt} \end{bmatrix} = \begin{bmatrix} -\frac{r_f}{L_f} & -\omega_e \\ \omega_e & -\frac{r_f}{L_f} \end{bmatrix} \begin{bmatrix} p_g \\ q_g \end{bmatrix} + \begin{bmatrix} u_{gd} \\ u_{gq} \end{bmatrix} \quad (19)$$

Where

$$u_{gd} = \frac{3}{2L_f}\left(v_s^2 - \left(v_{gd}v_{sd} + v_{gq}v_{sq}\right)\right)$$

$$u_{gd} = \frac{3}{2L_f}\left(v_{gq}v_{sd} - v_{gd}v_{sq}\right)$$

The dc-link model can be deduced as given by

$$V_{dc}(t)I_{dc}(t) = p_g(t) - p_r(t) - p_{loss}(t) \quad (20)$$

where $p_r(t)$ is the real power that the converter delivers to the rotor and p_{loss} represents the total power loss, including converter switching losses and copper losses of the filter.

The delivered real power to the rotor is

$$p_r = \frac{3}{2}\left(v_{rd}i_{rd} + v_{rq}i_{rq}\right).$$

Using (10) and (5), p_r can be expressed as

$$p_r = \frac{L_s\left(v_{sd}v_{rd} + v_{sq}v_{rq}\right)}{L_m|v_s|^2}p_s + \frac{L_s\left(v_{sq}v_{rd} - v_{sd}v_{rq}\right)}{L_m|v_s|^2} + \frac{3v_{rd}}{2L_m}\psi_{sd} + \frac{3v_{rq}}{2L_m}\psi_{sq}. \quad (21)$$

In the high-power converter, the power loss is often less than 1% of the total transferred power, and the impact of in p_{loss} (20) can be neglected. Substituting $I_{dc}(t) = C\left(dV_{dc}(t)\right)/(dt)$ in (20), the model of the dc link is deduced as follows:

$$\frac{dV_{dc}}{dt} = \frac{I_{dc}}{C} = \frac{p_g - p_r}{CV_{dc}}. \quad (22)$$

Using (21), the right-hand-side quantities in (22) can be expressed in terms of the state variables $p_s, q_s, P_g, \psi_{sq}, \psi_{sd}$.

D. Wind Turbine Model

The captured mechanical power by a wind turbine can be expressed with the algebraic aerodynamic equation as

$$P_m = \frac{1}{2}C_p(\lambda,\beta)\rho\pi R^2 V_w^3 \quad (23)$$

Where R, ρ, V_w are the wind turbine radius, air mass density, and wind speed, respectively. C_p is the wind turbine power coefficient which is a function of the tip speed ratio $\lambda = R\omega/V_\omega$ and the pitch angle of the turbine blades, β. For a high-power wind turbine, the maximum mechanical power captured at ranges from 6 to 8. Theoretically, it can be shown that C_p <0.6 and practically at $\lambda = \lambda_{opt}, C_P$ is about 0.5 for high-power wind turbines [1].

III. DFIG WIND TURBINE SEQUENTIAL LINEARIZED MULTIVARIABLE DYNAMIC MODEL

A. Modeling of DFIG and Wind Turbine

For a high-power machine, the stator resistant is small; therefore, based on (5), a constant stator voltage under normal operation yields slow-varying flux components. Thus, the dq components of the stator flux of a DFIG in a field-oriented frame of reference with $v_{sq} = 0$ can be obtained from (12) and (13) as

$$\psi_{sd} = 0, \psi_{sq} = -\frac{v_{sd}}{\omega_e}. \quad (24)$$

Substituting for $\psi_{sd,sq}$ from (31) in (10), (11), and (19), then by linearizing the equations about an operating point, the small signal model of DFIG can be expressed as

$$\frac{d\tilde{p}_s}{dt} = -g_1\tilde{p}_s - \omega_{s10}\tilde{q}_s + (q_{s0} + g_8)\tilde{\omega}_r + \tilde{u}_{rd}$$

$$\frac{d\tilde{q}_s}{dt} = \omega_{s10}\tilde{p}_s - g_1\tilde{q}_s - p_{s0}\tilde{\omega}_r + \tilde{u}_{rq}$$

$$\frac{d\tilde{\omega}_r}{dt} = -\frac{P^2}{J\omega_c}\tilde{p}_s - \frac{P}{J}\tilde{T}_m$$

Where ~ denotes small-signal quantities, and

$$g_8 = \frac{3v_{sd}^2}{2L_s'\omega_c}.$$

In the linearized model, superscript 0 denotes the quantities at an operating point. To calculate $\tilde{T}_m$, the power torque equation $P_m = T_m\omega_r$ is linearized by assuming a constant wind speed as

$$\tilde{T}_m = K_T\tilde{\omega}_r$$

Where K_T is obtained via linearizing P_m in (23) as given by

$$K_T \triangleq \left(\frac{1}{2}\rho\pi R^2 V_{\omega 0}^3\right)\left(\frac{R}{V_{\omega 0}\omega_{r0}}\frac{\partial C_p}{\partial}\right)$$

where is obtained via linearizing in (23) as given by Transferring the linearized dynamic model of DFIG and wind turbine in the Laplace domain yields

$$\begin{bmatrix} s+g_1 & \omega_{sl0} & -(q_{s0}+g_s) \\ -\omega_{sl0} & s+g_1 & p_{s0} \\ \frac{p^2}{j\omega_e} & 0 & s+\frac{pK_T}{J} \end{bmatrix}\begin{bmatrix}\tilde{p}_s \\ \tilde{q}_s \\ \tilde{\omega}_r\end{bmatrix} = \begin{bmatrix}\tilde{u}_{rd} \\ \tilde{u}_{rq} \\ 0\end{bmatrix} \quad (25)$$

Where

$$\tilde{u}_{rd} = g_2\tilde{v}_{rd}, \quad \tilde{u}_{rq} = -g_2\tilde{v}_{rq}$$

Using (37), the dynamic model of DFIG and the wind turbine in Laplace domain can be expressed based on a power transfer function as

$$\begin{bmatrix}\tilde{p}_s \\ \tilde{q}_s \\ \tilde{\omega}_r\end{bmatrix} = \begin{bmatrix} h_{11} & h_{12} \\ h_{21} & h_{22} \\ h_{31} & h_{32}\end{bmatrix}\begin{bmatrix}\tilde{u}_{rd} \\ \tilde{u}_{rq}\end{bmatrix} \quad (26)$$

Where h_{ij} can be readily obtained from the solution of (37) for $\tilde{p}_s, \tilde{q}_s$ and $\tilde{\omega}_r$.

B. Model of the Grid-Side Filter and DC Link

The model of the grid-side filter in Laplace domain can be obtained by transferring (23) into the Laplace domain as

$$\begin{bmatrix} s+\frac{rf}{lf} & \omega e \\ -\omega e & s+\frac{rf}{lf}\end{bmatrix}\begin{bmatrix}\tilde{p}_g \\ \tilde{q}_g\end{bmatrix} = \begin{bmatrix}\tilde{u}_{gd} \\ \tilde{u}_{gd}\end{bmatrix} \quad (27)$$

Where

$$\tilde{u}_{gd} = -\frac{3v_{sd}}{2L_f}\tilde{v}_{gd}, \quad \tilde{u}_{gq} = \frac{3v_{sd}}{2L_f}\tilde{v}_{gq}$$

Solving (27) for $\tilde{p}_g$ and $\tilde{q}_g$, the grid-side filter model in the Laplace domain is

$$\begin{bmatrix}\tilde{p}_g \\ \tilde{q}_g\end{bmatrix} = \begin{bmatrix} g_{11} & g_{12} \\ g_{21} & g_{22}\end{bmatrix}\begin{bmatrix}\tilde{u}_{gd} \\ \tilde{u}_{gq}\end{bmatrix} \quad (28)$$

Where

$$g_{11} = g_{22} = \frac{s+\frac{R_f}{L_f}}{\left(s+\frac{R_f}{L_f}\right)+\omega_e^2}$$

$$g_{12} = -g_{21} = \frac{-\omega_e}{\left(s+\frac{R_f}{L_f}\right)+\omega_e^2}$$

Using (22), the linearized model of dc link can be obtained as

$$\frac{d\tilde{v}_{dc}}{dt} = \frac{\tilde{p}_g - \tilde{p}_r}{CV_{dc0}} \quad (29)$$

Where

$$\tilde{p}_r = \propto_1 \tilde{p}_s + \propto_2 \tilde{q}_s + \propto_3 \tilde{u}_{rd} + \propto_4 \tilde{u}_{rq} \quad (30)$$

$$\propto_1 = \frac{L_s v_{rd0}}{L_m v_{sd}}, \quad \propto_2 = \frac{L_s v_{rq0}}{L_m v_{sd}},$$

$$\propto_3 = \frac{2L_s^2 L_r' p_{s0}}{3L_m^2 v_{sd}^2}, \propto_4 = \left(\frac{L_s' L_r}{L_m^2\omega_e} + \frac{2L_s^2 L_r' q_{s0}}{3L_m^2 v_{sd}^2}\right)$$

From (29), the dc bus model in the Laplace domain is

$$\tilde{V}_{dc} = \frac{\tilde{p}_g - \tilde{p}_r}{sCV_{dc0}} \quad (31)$$

Equations (26), (28), and (31) represent the linearized multivariable model of a DFIG wind turbine generator.

IV. CONTROLLER DESIGN SCHEME

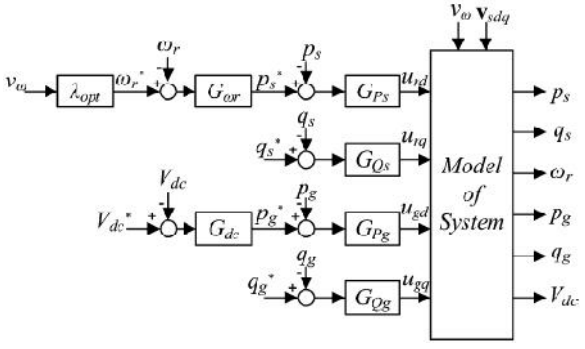

Fig.3: Multi variable feedback control system for the rotor side and grid side converters

Fig. 3 demonstrates the suggested multivariable feedback control system for the machine- and grid-side control schemes. In this scheme, the control inputs of the linearized model of the system are (u_{rd}, u_{rq}) to control real/reactive power of the rotor; and (u_{gd}, u_{gq}) to adjust the dc-link voltage and injected reactive power to the system. The outputs (feedbacks) of the system are the rotor speed, dc-link voltage, and the instantaneous real/reactive power of the rotor- and grid-side converters. The feedback control system includes six compensators which are used in two nested loops. The inner loops consist of G_{Ps}, G_{Qs}, G_{Pg} and G_{Qg} where the required reactive power of the machine and grid are directly controlled via G_{Qs} and G_{Qg} control loops as shown Fig. 3. The outer control loops include $G_{\omega r}$ for regulating the rotor speed and G_{dc} for adjusting the dc-link voltage level. The sequential loop closing (SLC) method [17] is adopted to design six controllers based on the multivariable model of the system developed in Section III. Based on the theory of the SLC design method [17], the multivariable system is stable if all of the designed subsystems during the sequential controller design procedure are stable.

A. Design of the Rotor-Side Controllers

1) Stator Real and Reactive Power Controllers: $(\tilde{u}_{rd}, \tilde{P}_s)$ Considering as the first pair in (26) and, thus, imposing $u_{rq} = 0$, we obtain the first SISO subsystem for controller design as

$$\tilde{p}_s = h_{11}\tilde{u}_{rd} \tag{32}$$

The first controller to be designed is

$$\tilde{u}_{rd} = G_{Ps}(\tilde{p}_s^* - \tilde{p}_s) \tag{33}$$

Substituting from (49) in (48), the closed-loop model of the first subsystem in Laplace domain is

$$\tilde{p}_s = \frac{h_{11}G_{Ps}}{1+h_{11}G_{Ps}}\tilde{p}_s^* \tag{34}$$

Thus, G_{Ps} must be designed so that all poles of (34) remain in the left-half plane (LHP). The design of G_{Ps} can be simply performed via SISO system design methods, such as frequency response or root locus. To design G_{Qs} for reactive power control, the first controller G_{Ps} is considered as a part of the system, and then by substituting for $\tilde{u}_{rd} = G_{Ps}(\tilde{p}_s^* - \tilde{p}_s)$ and $\tilde{u}_{rq} = G_{Qs}(\tilde{q}_s^* - \tilde{q}_s)$ in (26), the closed-loop model of the second subsystem is obtained

$$\tilde{q}_s = \frac{G_1}{1+G_2G_{Qs}}\tilde{p}_s^* + \frac{G_1G_{Qs}}{1+G_2G_{Qs}}\tilde{q}_s^* \tag{35}$$

Where

$$G_1 = \frac{h_{21}G_{Ps}}{1+h_{11}G_{Ps}}, \quad G_2 = h_{22} - \frac{h_{12}h_{21}G_{Ps}}{1+h_{11}G_{Ps}}$$

Thus, G_{Qs} must be designed so that the second subsystem in (35) remains stable.

2) Rotor Speed Controller: Speed control of the turbine-generator rotor is performed via control of the real power of the stator. Therefore, the speed controller uses $G_{\omega r}$ as the control input. Using the control scheme of Fig. 3, $\tilde{p}_s^*$ is

$$\tilde{p}_s^* = G_{\omega r}(\omega_r^* - \tilde{\omega}_r) \tag{36}$$

Embedding G_{Ps} and G_{Qs} controllers in the model of the system, the transfer function of rotor speed can be calculated as

$$\tilde{\omega}_r = G_3P_s^* + G_4\tilde{q}_s^* \tag{37}$$

Substituting for P_s^* from (52) in (53) yields
Where

$$G_3 = \frac{h_{31}G_{Ps}\left(1 + G_{Qs}(G_1 + G_2)\right)}{(1 + h_{11}G_{Ps})(1 + G_2G_{Qs})} - \frac{h_{32}G_{Qs}G_1}{(1 + G_2G_{Qs})}$$

$$G_4 = \frac{h_{32}G_{Qs}}{1 + G_2G_{Qs}} - \frac{h_{12}h_{31}G_{Ps}^2}{(1 + h_{11}G_{Ps})(1 + G_2G_{Qs})}$$

$$\tilde{\omega}_r = \frac{G_3G_{\omega r}}{1+G_3G_{\omega r}}\tilde{\omega}_r^* + \frac{G_4}{1+G_3G_{\omega r}}\tilde{q}_s^* \tag{38}$$

Thus, $G_{\omega r}$ must be designed so that the subsystem in (38) remains stable.

B. Grid-Side Controller

1) Grid-Side Power Controllers: The controller design procedure for G_{Pg} and G_{Qg} is quite similar to that of the rotor-side converter since both controllers have the same structure. Therefore, G_{Pg} and G_{Qg} can be simply obtained by repeating the design procedure as explained in (32) – (35). The only modification is replacing h_{ij} $(i,j=1,2)$ with g_{ij} $(i,j=1,2)$. Also, both subscripts and should be replaced with subscript *s* and *r*.

2) DC-Link Voltage Controller: Substituting for p_s, q_s, u_{rd} , and u_{rq} into (30), we obtain

$$\tilde{p}_r = \frac{G_5 G_{\omega r}}{1+G_3 G_{\omega r}} \tilde{\omega}_r^* + \left(G_6 - \frac{G_3 G_5 G_{\omega r}}{1+G_3 G_{\omega r}}\right) \tilde{q}_s^* \quad (39)$$

where detailed expressions for G_5 and G_6 are given in the Appendix. Based on (31) and (39), p_g^* can regulate at its reference value using the dc-link controller G_{dc} in $\tilde{p}_g^* = G_{dc}(\tilde{V}_{dc}^* - \tilde{V}_{dc})$. Therefore, the closed-loop system for V_{dc} is deduced as

$$\tilde{V}_{dc} = \frac{G_7 G_{dc} \tilde{V}_{dc}^* + G_8 \tilde{q}_g^*}{sCV_{dc0} + G_7 G_{dc}} - \frac{G_5 G_{\omega r} \tilde{\omega}_r^* + (G_6 + G_3 G_{\omega r}(G_6 - G_5)) \tilde{q}_s^*}{(sCV_{dc0} + G_7 G_{dc})(1+G_3 G_{\omega r})} \quad (40)$$

where detailed expressions for G_7 and G_8 are given in the Appendix. Finally, G_{dc} must be designed to stabilize the dc-link closed-loop system in (40).

D. Fault ride through by current limiting

The target of the controller design procedure mainly deals with stability, tracking performance for capturing maximum wind power, disturbance rejection, and robustness against uncertainties and unaccounted dynamics.

The main attention in the paper is, therefore, drawn to the control of the DFIG wind turbine and of its power converter and to the ability to protect itself without disconnection during grid faults. The paper provides also an overview on the interaction between variable-speed DFIG wind turbines and the power system subjected to disturbances. During a fault and/or sever transients, additional protection algorithms, such as fault ride through (FRT) and startup algorithms, must be added to the control system. Various algorithms, including active crowbar [18], series dynamic restorer, and dynamic voltage restorer have been suggested for FRT. These algorithms are independent of the control approach during the normal operation; therefore, they can be used with the proposed transfer power matrix method herein as well.

V. SIMULATION STUDY OF THE MULTIVARIABLE DFIG WIND TURBINE CONTROL SYSTEM

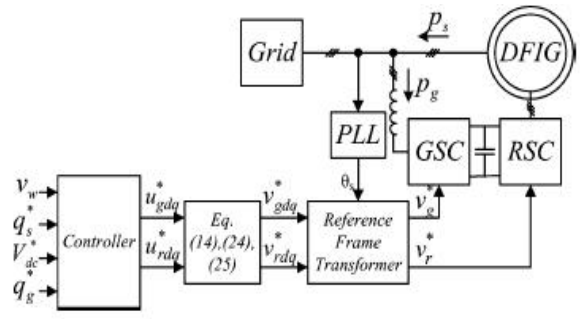

Fig. 4. Block diagram of the study system.

The test system of DFIG wind turbine is as shown in Fig. 4. The study system includes a 1.5-MW DFIG wind turbine-generator connected to a grid. In this paper SVPWM method is used for better controlling of converters. The electrical and mechanical parameters of the turbine generator summarized in Table I [24]. The following per-unitized controllers were designed for the study system by using proposed method of design

$$G_{Ps} = 1.33\left(1 + \frac{10}{s} + \frac{s}{166.25}\right)\left(\frac{1}{1+0.016s}\right)$$

$$G_{Qs} = 2.65\left(1 + \frac{10}{s} + \frac{s}{331.25}\right)\left(\frac{1}{1+0.0032s}\right)$$

$$G_{Pg} = 2.65\left(1 + \frac{10}{s}\right), \quad G_{Qg} = 2.65\left(1 + \frac{10}{s}\right)$$

$$G_{dc} = 4.32\left(1 + \frac{2}{s}\right), \quad G_{\omega r} = 7.54\left(1 + \frac{2}{s}\right)$$

The performance of these controllers was evaluated by using time-domain simulation of the study system using the Matlab/ Simulink software tool.

The selected wind speed pattern spans an input mechanical wind power from 0.7 to 1 p.u. (70 to 100% of the turbine-generator rated power). This selected pattern gives the trapezoidal behavior of the wind speed.

The reactive power command is a step change of 0.25 p.u. and occurs at t=3 s when the real power is about 0.6 p.u.

A. Tracking and Disturbance Rejection Capabilities

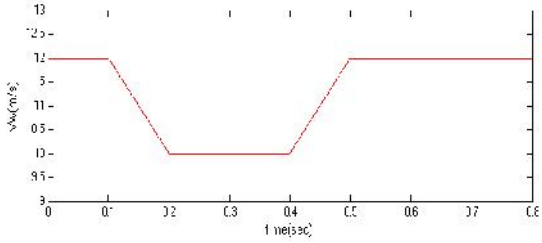

Fig. 5 Trapezoidal pattern for wind speed

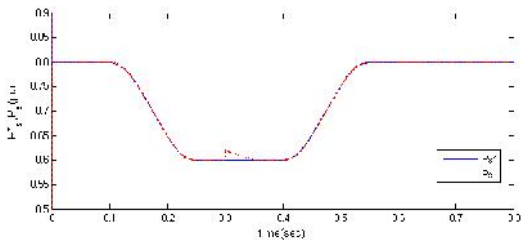

(a)

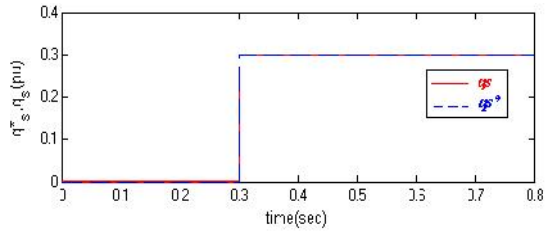

(b)

Fig. 6. Tracking performance of (a) real and (b) reactive stator powers.

TABLE I
STUDY SYSTEM'S WIND GENERATOR DATA

PARAMETERS	VALUES	UNITS
Rated Power	1.5	[MW]
Rated Voltage (Line-to-Line)	0.575	[kV]
Rated Frequency	60	[Hz]
Rated Wind Speed	12.0	[m/s]
Stator resistance	1.4	[mΩ]
Rotor resistance	0.99	[mΩ]
Stator leakage inductance	89.98	[μH]
Rotor leakage inductance	82.08	[μH]
Magnetization inductance	1.526	[mH]
Stator/rotor turns ratio	1	-
Poles	6	-
Turbine rotor diameter	70	[m]
Lumped inertia constant	5.04	[s]

Fig. 6 shows the real/reactive power tracking of the DFIG against the disturbances present in the given wind speed pattern. Because of the coupling all powers are interlinked to each other. This coupling effect is also shown in the fig. 6(a) at t=3s. At this instant i.e., at t=3s the step change in reference reactive power causes the small deviation in the real power because of the coupling phenomenon. Finally from fig. 6 the controller scheme eliminating the coupling effect impact while tracking the command signals.

Fig. 7(a) and (b) describes the dc-link voltage and the rms values of the machine voltage/current quantities. These figures show that the stator and rotor currents are changing as the real/reactive power changes whereas the dc link and stator voltages remained fixed as expected from the control strategy.

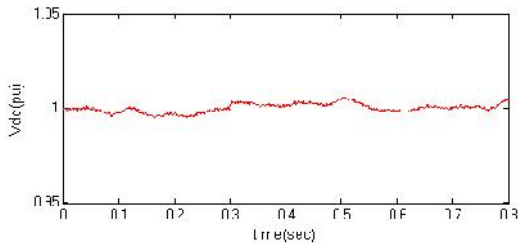

(a)

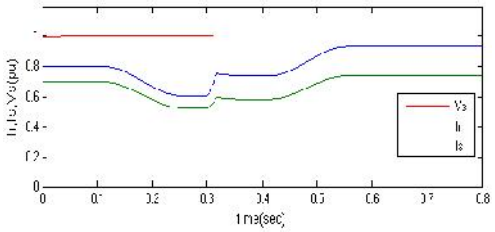

(b)

Fig. 7. RMS values of the (a) stator voltage and (b) currents.

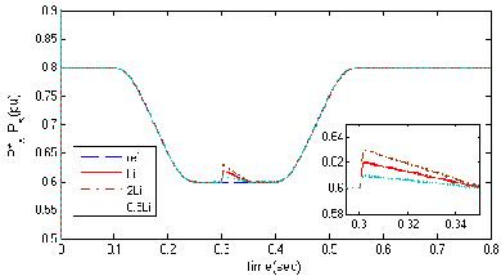

(a)

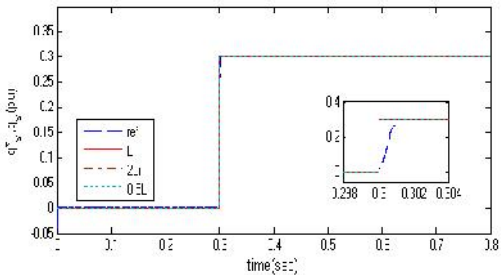

(b)

Fig. 8. Robustness of the controllers to variations in L_l.

B. Control System Robustness

Fig. 8 evaluates the performance of tracking reference powers and avoiding the disturbances when the leakage inductance of the machine L_l is changed to twice ($2L_l$) and reduced to half ($0.5L_l$). So the proposed method gives the robustness of the control system designed.

VI. CONCLUSION

A new SVPWM based approach for modeling and control using power transfer matrix is evaluated in this paper for a study of DFIG wind turbine to control real/ reactive power at both rotor and grid sides. This multi variable sequential feedback control system approach gives the stability in the case of fault condition in the converter and unbalanced condition. The proposed method validated through time domain simulation by using

MATLAB/Simulink software and the results validates the system robustness. The results shows that the suggested model and control scheme can successfully track the rotor speed reference for capturing the maximum power and maintain the dc-link voltage of the converter regardless of disturbances due to changes in real and reactive power references.

APPENDIX

Details of G_5, G_6, G_7 and G_8 in (39) and (40) are shown in the equations below

$$G_5 = \frac{G_1(\alpha_2 - \alpha_4 G_{Qs})}{1 + G_2 G_{Qs}} + \alpha_3 G_{Ps} + \frac{(\alpha_1 - \alpha_3 G_{Ps})(h_{11} G_{Ps}(1 + G_2 G_{Qs}) - h_{12} G_1 G_{Qs})}{(1 + h_{11} G_{Ps})(1 + G_2 G_{Qs})}$$

$$G_6 = \frac{h_{12} G_{Ps}(\alpha_1 - \alpha_3 G_{Ps})}{(1 + h_{11} G_{Ps})(1 + G_2 G_{Qs})} + \frac{G_2 G_{Qs}(\alpha_2 - \alpha_4 G_{Qs})}{1 + G_2 G_{Qs}} + \alpha_4 G_{Qs}$$

$$G_7 = \frac{g_{21} G_{Ps}}{1 + g_{11} G_{Ps}} \left(\frac{g_{11}}{g_{12}} + \frac{g_{21}}{g_{12}} G_0 \right)$$

$$G_8 = \frac{g_{12} G_{Qs}}{1 + (g_{11} + g_{21}^2) G_{Ps} + g_{11} G_{Qs} + g_{11}^2 G_{Ps} G_{Qs}}.$$

REFERENCES

[1] M. Patel, *Wind and Solar Power Systems: Design, Analysis, and Operation*. Boca Raton, FL: CRC, 2006.

[2] T. Zhou and B. François, "Energy management and power control of a hybrid active wind generator for distributed power generation and grid integration," *IEEE Trans. Ind. Electron.*, vol. 58, no. 1, pp. 95–104, Jan. 2011.

[3] J. Hu, H. Nian, H. Xu, and Y. He, "Dynamic modeling and improved control of DFIG under distorted grid voltage conditions," *IEEE Trans. Energy Convers.*, vol. 26, no. 1, pp. 163–175, Mar. 2011.

[4] E. Tremblay, S. Atayde, and A. Chandra, "Comparative study of control strategies for the doubly fed induction generator in wind energy conversion systems:ADSP-based implementation approach," *IEEE Trans. Sustain. Energy*, vol. 2, no. 3, pp. 288–299, Jul. 2011.

[5] M. Mohseni, S. Islam, and M. Masoum, "Enhanced hysteresis-based current regulators in vector control of DFIG wind turbines," *IEEE Trans. Power Electron.*, vol. 26, no. 1, pp. 223–234, Jan. 2011.

[6] Z.Wang, G. Li, Y. Sun, and B. Ooi, "Effect of erroneous position measurements in vector-controlled doubly fed induction generator," *IEEE Trans. Energy Convers.*, vol. 25, no. 1, pp. 59–69, Mar. 2010.

[7] P. Rodríguez, A. Luna, I. Candela, R. Mujal, R. Teodorescu, and F. Blaabjerg, "Multiresonant frequency-locked loop for grid synchronization of power converters under distorted grid conditions," *IEEE Trans.Ind. Electron.*, vol. 58, no. 1, pp. 127–138, Jan. 2011.

[8] G. Escobar, M. Martinez-Montejano, A. Valdez, P. Martinez, and M. Hernandez-Gomez, "Fixed reference frame phase-locked loop (FRF-PLL) for grid synchronization under unbalanced operation," *IEEE Trans. Ind. Electron.*, vol. 58, no. 5, pp. 1943–1951, May 2011.

[9] R. Datta and V. Ranganathan, "Direct power control of grid-connected wound rotor induction machine without rotor position sensors," *IEEE Trans. Power Electron.*, vol. 16, no. 3, pp. 390–399, May 2001.

[10] S. Chen, N. Cheung, K. Wong, and J. Wu, "Integral sliding-mode direct torque control of doubly-fed induction generators under unbalanced grid voltage," *IEEE Trans. Energy Convers.*, vol. 25, no. 2, pp. 356–368, Jun. 2010.

[11] S. Chen, N. Cheung, K. Wong, and J. Wu, "Integral variable structure direct torque control of doubly fed induction generator," *IET Renew. Power Gen.*, , vol. 5, no. 1, pp. 18–25, 2011.

[12] D. Zhi, L. Xu, and B. Williams, "Model-based predictive direct power control of doubly fed induction generators," *IEEE Trans. Power Electron.*, vol. 25, no. 2, pp. 341–351, Feb. 2010.

[13] P. Zhou, W. Zhang, Y. He, and R. Zeng, "Improved direct power control of a grid-connected voltage source converter during network unbalance," *J. Zhejiang Univ.-Sci. C*, vol. 11, no. 10, pp. 817–823, 2010.

[14] J. Hu, H. Nian, B. Hu, Y. He, and Z. Zhu, "Direct active and reactive power regulation of DFIG using sliding-mode control approach," *IEEE Trans. Energy Convers.*, vol. 25, no. 4, pp. 1028–1039, Dec. 2010.

[15] P. Krause, O. Wasynczuk, S. Sudhoff, and I. P. E. Society, *Analysis of Electric Machinery and Drive Systems*. Piscataway, NJ: IEEE, 2002.

[16] A. Tabesh and R. Iravani, "Multivariable dynamic model and robust control of a voltage-source converter for power system applications," *IEEE Trans. Power Del.*, vol. 24, no. 1, pp. 462–471, Jan. 2009.

[17] J. Maciejowski, *Multivariable Feedback Design*, ser. Electron. Syst. Eng. Ser. Reading , MA: Addison-Wesley, 1989, vol. 1.

[18] C. Wessels, F. Gebhardt, and F. Fuchs, "Fault ride-through of a DFIG wind turbine using a dynamic voltage restorer during symmetrical and asymmetrical grid faults," *IEEE Trans. Power Electron.*, vol. 26, no. 3, pp. 807–815, Mar. 2011.

GONDI SWATHI currently pursuing her M.Tech in Power Electronics and Industrial drives from QIS Institute of Technology, Ongole, Andhra Pradesh, India affiliated to JNTU University, Kakinada. She has done her B.Tech degree from Malineni Lakshmaiah Enginerring College, affiliated to JNT University, Kakinada, Andhra Pradesh, India and her fields of interest include Power Systems.

Prof. O.V.S.SRINIVASA PRASAD received the B.E degree Instrumentation Engineering from AU college of engineering, Andhra University, Visakapatnam, the M.E degree in Power Electronics from Gulbarga university, Karnataka state and he was currently working as Professor and HOD of EEE department at Qis institute of technology, Affiliated to JNTUK university, Kakinada, East Godavari (dst), Andhra Pradesh, India.

A. VENKATA SURESH currently working as Associate professor in department of EEE, QIS Institute of Technology ongole, A.P. He did his B.Tech (EEE) in malineni lakshmaiah engineering college JNTUH, ongole, AP and M.Tech in Electrical Power systems in QISCEET JNTU Kakinada. His main working area includes power quality and FACTS.